Combinatorial gene therapy accelerates bone regeneration: non-viral dual delivery of VEGF and BMP2 in a collagen-nanohydroxyapatite scaffold.

AUTHOR(S)

Caroline Curtin, Erica G. Tierney, Kevin McSorley, Sally-Ann Cryan, Garry Duffy, Fergal O'Brien

Combinatorial Gene Therapy Accelerates Bone Regeneration: Non-viral Dual Delivery of VEGF and BMP2 in a Collagen-nanohydroxyapatite Scaffold

Caroline M. Curtin[1, 2, 3†], Erica G. Tierney[1, 2, 3†], Kevin McSorley[1], Sally-Ann Cryan[4], Garry P. Duffy[1, 2, 3], Fergal J. O'Brien[1, 2, 3*]

[1] Tissue Engineering Research Group, Dept. of Anatomy, Royal College of Surgeons in Ireland, Dublin, Ireland

[2] Trinity Centre for Bioengineering, Trinity College Dublin, Dublin, Ireland

[3] Advanced Materials and BioEngineering Research (AMBER) Centre, Royal College of Surgeons in Ireland & Trinity College Dublin, Dublin 2, Ireland

[4] School of Pharmacy, Royal College of Surgeons in Ireland, Dublin, Ireland

†These authors contributed equally to this work.

*Corresponding author. E-mail: fjobrien@rcsi.ie

Non-viral delivery of single genes combined with biomaterial scaffolds is increasingly showing potential in tissue engineering. In this study, we developed a bioactive, collagen nano-hydroxyapatite (coll-nHA) scaffold as a dual gene delivery platform *in vitro* and *in vivo*. Firstly, the ability of nHA particles, developed in-house, and polyethylenimine (PEI) to act as non-viral vectors for delivery of bone morphogenetic protein 2 (pBMP2) and vascular endothelial growth factor (pVEGF), pro-osteogenic and pro-angiogenic genes respectively, was determined in mesenchymal stem cells (MSCs). nHA and PEI were then combined with the genes in various combinations with coll-nHA scaffolds to produce a scaffold highly conducive to the production of vascularised bone. These dual combinatorial pVEGF/pBMP2 gene-activated scaffolds demonstrated superior MSC-mediated osteogenesis *in vitro* and increased vascularisation and bone repair by host cells *in vivo*. Ultimately, the use of nHA to deliver both pVEGF and pBMP2 markedly accelerated bone healing with a 36-fold increase in bone formation in the nHA dual scaffold versus the empty defect as early as 4 weeks post-implantation underlining its immense potential in bone regeneration.

Although bone can regenerate following fracture, large bone defects have limited capacity for repair and as such require alternative strategies. Tissue-engineered scaffolds are promising alternatives to bone grafts as they can provide both a functional three-dimensional template that houses cells and, in addition, can be designed to facilitate the controlled release of recombinant proteins or genes to enhance healing. The use of proteins is associated with limitations including high cost, bolus release

of protein, short half-life, and the large doses needed to achieve a therapeutic effect. Gene-activated scaffolds are a new avenue of research and consist of biomaterial scaffolds functionalised to act as depots for gene delivery while simultaneously offering structural support and a matrix for new tissue deposition. A gene-activated scaffold can therefore induce the body's own cells to steadily produce specific proteins providing a much more efficient alternative.

The dual delivery of therapeutic proteins or genes may have increased regenerative potential over the delivery of single proteins or genes [1, 2] and although dual delivery scaffolds have previously been developed, they typically deliver proteins [3-5]. The next generation gene-activated scaffold might therefore include multiple genes to promote synergistic cell-mediated protein production. In bone repair, neo-vascularisation of the damaged bone is critical to the healing outcome. Therefore a dual scaffold containing an angiogenic gene to promote vascularisation combined with an osteogenic gene may enhance bone repair. Few *in vitro* gene delivery systems providing co-expression of therapeutic genes have been demonstrated using multi-gene combinations [6-8] and to our knowledge, no bone-targeted scaffold containing different non-viral vectors carrying alternate therapeutic genes has been reported. This study thus focused on the development of a combinatorial dual gene-activated scaffold to deliver two different genes - pVEGF and pBMP2. BMP2 is well known for its therapeutic capacity for bone repair [9-11] while VEGF is typically used for vascularisation. A small number of *in vitro* and *in vivo* studies have reported the synergistic effects of dual VEGF and BMP2 protein delivery relative to singular systems [3, 4, 12].

Non-viral vectors were utilised in the development of these scaffolds to overcome safety problems associated with viral vectors such as insertional mutagenesis [13] and adverse immune responses [14]. Recently within our laboratory, polyethyleneimine (PEI) has been optimised as a vector within collagen-based scaffolds demonstrating efficacy with a high transfection efficiency and uncompromised cell viability [15, 16]. In addition, in-house synthesised nano-hydroxyapatite (nHA), which was initially used to improve the mechanical properties and osteogenic potential of the scaffolds, [17] was also recently adapted in our lab as a vector for MSC transfection [18] where significantly elevated levels of MSC-mediated mineralisation were observed in nHA-pBMP2 coll-nHA scaffolds [18].

The hypothesis of this study is that a multi-faceted approach of a scaffold optimised for bone repair containing osteogenic and angiogenic genes delivered with individual non-viral vectors tailored for transfection of MSCs would have immense potential for bone repair. Therefore, the overall goal of this study was initially to establish the optimal vector for the delivery of pVEGF and pBMP2

individually before incorporating both in a combinatorial dual scaffold to promote MSC-mediated osteogenesis *in vitro* and increased host-mediated vascularisation and bone repair *in vivo*.

Firstly, the respective transfection efficiencies of the PEI and nHA vectors were determined using the reporter gene plasmid Green Fluorescent Protein (pGFP) and compared to nucleofection as a positive control (Fig 1a). Nucleofection led to the highest levels of transfection with a gene transfer efficiency of 80.1 ± 9.3% and PEI yielded higher levels of transfection (30.4 ± 8.4%) than nHA (11.5± 1.3%).

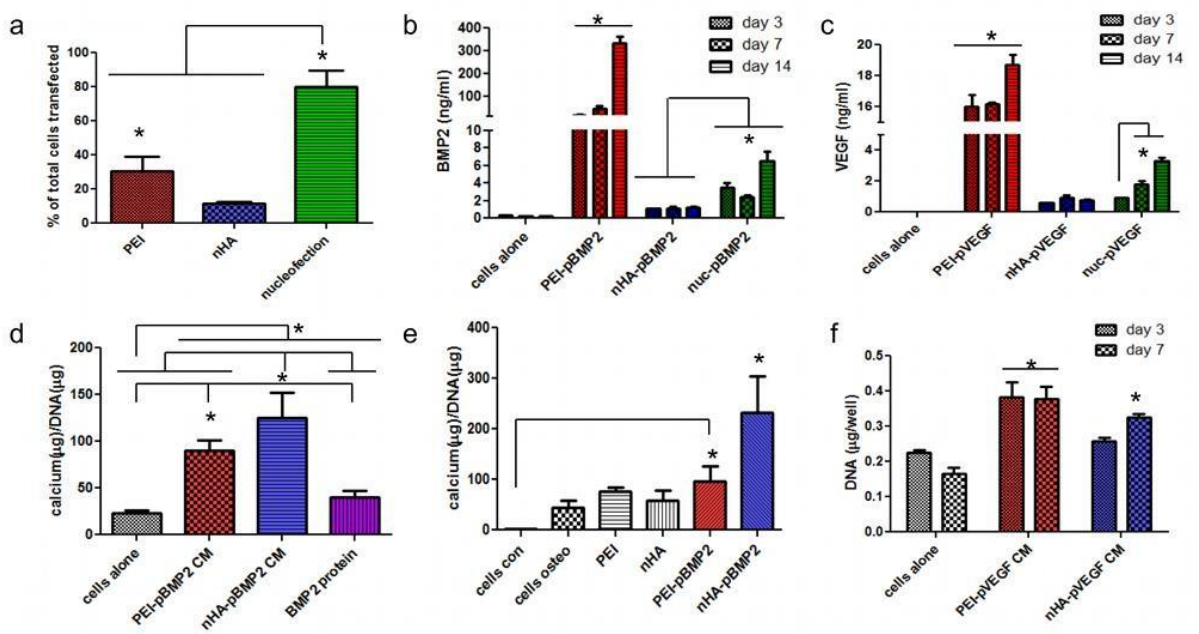

Figure 1. nHA and PEI result in enhanced delivery of functional BMP2 and VEGF to MSCs. a, Nucleofection promotes the most effective transfection followed by PEI. b, BMP2 production was highest following PEI transfection. c, Similarly, the highest VEGF production occurred following PEI transfection. d, Increased osteoblast differentiation was observed when treated with media taken from PEI-pBMP2 and nHA-pBMP2 transfected cells in comparison to the addition of recombinant BMP2 protein. e, Enhanced calcium/DNA content was obtained in the nHA-pBMP2 transfected group compared to all other groups analysed. Enhanced proliferation of endothelial cells was observed when treated with media taken from PEI-pVEGF or nHA-pVEGF transfections. *p ≤0.05

MSCs were then transfected/nucleofected with pBMP2 to analyse the ability of each vector to elicit functional BMP2 production. All vectors successfully led to the production of BMP2 protein (Fig. 1b) but PEI-pBMP2 transfection induced remarkably higher levels of BMP2 production. Although PEI-pGFP expression was almost 3-fold lower than nucleofection, PEI-pBMP2 expression exceeded nucleofection. Similarly, MSCs were transfected/nucleofected with pVEGF where all vectors increased VEGF protein expression but cells transfected with PEI-pVEGF again induced the highest levels of VEGF expression (Fig. 1c). In order to verify the bioactivity of this BMP2, media from the

transfected MSCs was added to pre-osteoblasts and calcium deposition was measured (Fig. 1d). Interestingly, the nHA-pBMP2 group had significantly increased calcium/DNA deposition relative to all other groups (Fig. 1d). Moreover, the addition of both nHA-pBMP2 media and PEI-pBMP2 media from transfected cells promoted significantly higher calcium deposition compared to the addition of 50ng/ml of recombinant BMP2 protein (recommended dose). This indicates that the BMP2 levels produced using non-viral gene therapy were more effective than the direct addition of BMP2 recombinant protein – the current clinical standard. Osteogenic assays performed on the transfected MSCs showed that nHA-pBMP2 transfected MSCs produced statistically higher levels of calcium/DNA than all other groups indicating that nHA-pBMP2 provides levels of BMP2 conducive to enhanced osteogenesis (Fig. 1e). Of particular note is that the very high levels of BMP2 expression seen with PEI-pBMP2 transfected cells did not translate into higher levels of calcium suggesting high levels of BMP2 expression may not directly translate to increased osteogenesis and thus therapeutic potential. As endothelial cells proliferate in response to the addition of VEGF, VEGF functionality was analysed by adding media from pVEGF-transfected MSCs to endothelial cells (HUVECs; Fig. 1f). At day 3, the levels of DNA measured in the PEI-pVEGF group was significantly higher than the nHA-pVEGF group and endothelial cells alone. However, at day 7 both vectors increased endothelial cell proliferation relative to the cells alone control indicating that both vectors are suitable for pVEGF delivery and therefore for enhancing angiogenesis while suggesting that PEI is superior.

Having characterised protein expression and osteogenesis in monolayer culture, the pDNA-vector complexes were applied to scaffolds in various combinations as outlined in Fig. 2a, i.e. the PEI dual (PEI-pVEGF/PEI-pBMP2), nHA dual (nHA-pVEGF/nHA-pBMP2) and a mix dual gene-activated scaffold (composed of PEI-pVEGF and nHA-pBMP2 based on the optimal gene vectors derived from monolayer *in vitro* experiments), to assess their potential. All three dual scaffolds were shown to augment MSC-mediated calcium deposition and mineralisation *in vitro* after only 14 days. MicroCT images and alizarin red staining (Fig. 2b) showed marked increases in calcium production in the nHA dual and particularly the mix dual scaffold. Calcium quantification confirmed that both the mix dual scaffold and nHA dual scaffold induced the highest levels calcium deposition (Fig. 2c). The lower levels of mineralisation observed in the PEI dual scaffold despite the high levels of VEGF and BMP2 production was an unanticipated finding indicating that excessive amounts of protein production may actually deter osteogenesis. Ultimately, the enhanced osteogenesis observed in both the nHA and mix dual scaffold was very encouraging. Subsequently, gene-activated scaffolds containing pGFP complexed with either PEI or nHA were implanted in a rat cranial defect where the presence of GFP expressing cells confirmed the capability of these scaffolds to recruit and transfect host cells *in vivo* (Fig. 2d).

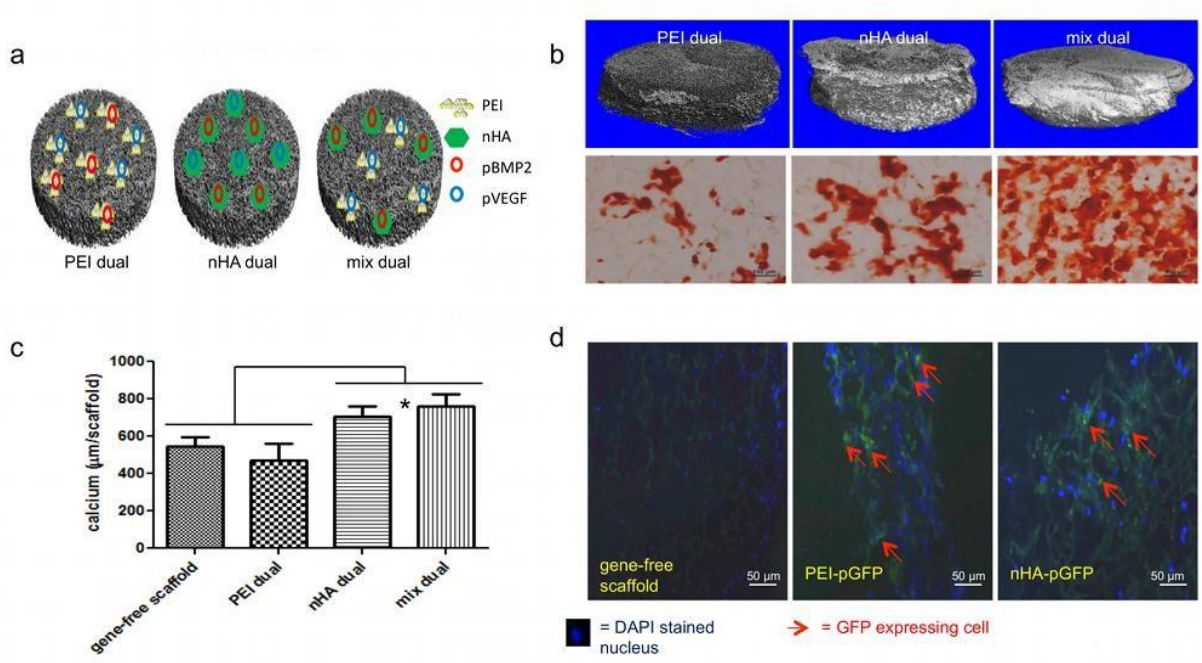

Figure 2. Development of functional dual gene-activated scaffolds for *in vitro* and *in vivo* gene delivery. a, Schematic of dual pVEGF-pBMP2 scaffolds. b, Reconstructed microCT images and alizarin red staining of dual scaffolds. c, Quantification showed that the mix dual and nHA dual scaffold enhanced osteogenesis relative to the gene-free and the PEI dual scaffold. d, GFP-expressing cells were observed in pGFP scaffolds implanted in a rat cranial defect for 1 week. *p ≤0.05

Following *in vitro* confirmation of their enhanced osteogenic potential and confirmation of successful *in vivo* transfection of host cells, the ability of the therapeutic dual scaffolds to promote vascularisation and bone repair was assessed in a rat critical-sized cranial defect model. Qualitative microCT and histological analysis revealed that all combinatorial dual scaffolds contributed to enhanced tissue healing as noted in Fig. 3. However, the nHA dual scaffold displayed the most advanced healing profile with good cell infiltration, large areas of deeply stained bone nucleation sites, and good integration at the interface between the scaffold and the defect edge (Fig 3a). Quantitative microCT analysis (Fig. 3b) showed that it produced higher percentage bone volume/tissue volume (BV/TV) than all other groups. The mix dual scaffold also induced a significantly pronounced healing response and while the PEI dual scaffold did not statistically augment bone volume in the defect site relative to the gene-free scaffold, it did elicit an enhanced response when compared to the empty defect control. Histomorphometrical analysis corroborated these results (Fig. 3c). Measurement of new bone formation revealed significantly higher levels of new bone in the nHA dual scaffold, the mix dual scaffold contained the next highest levels, the PEI dual scaffold induced more bone than the gene-free scaffold and finally, the gene-free scaffold induced more than the empty defect. In order to further understand the mechanism for accelerated bone regeneration, vessel formation was analysed (Fig. 3d-e). The mix dual scaffold contained

significantly more vessels than the empty defect and interestingly, the nHA dual scaffold had more vessels than any other group. It is likely therefore that the higher levels of VEGF produced by cells transfected in the mix dual scaffold and the nHA dual scaffold are responsible for this increased vessel formation.

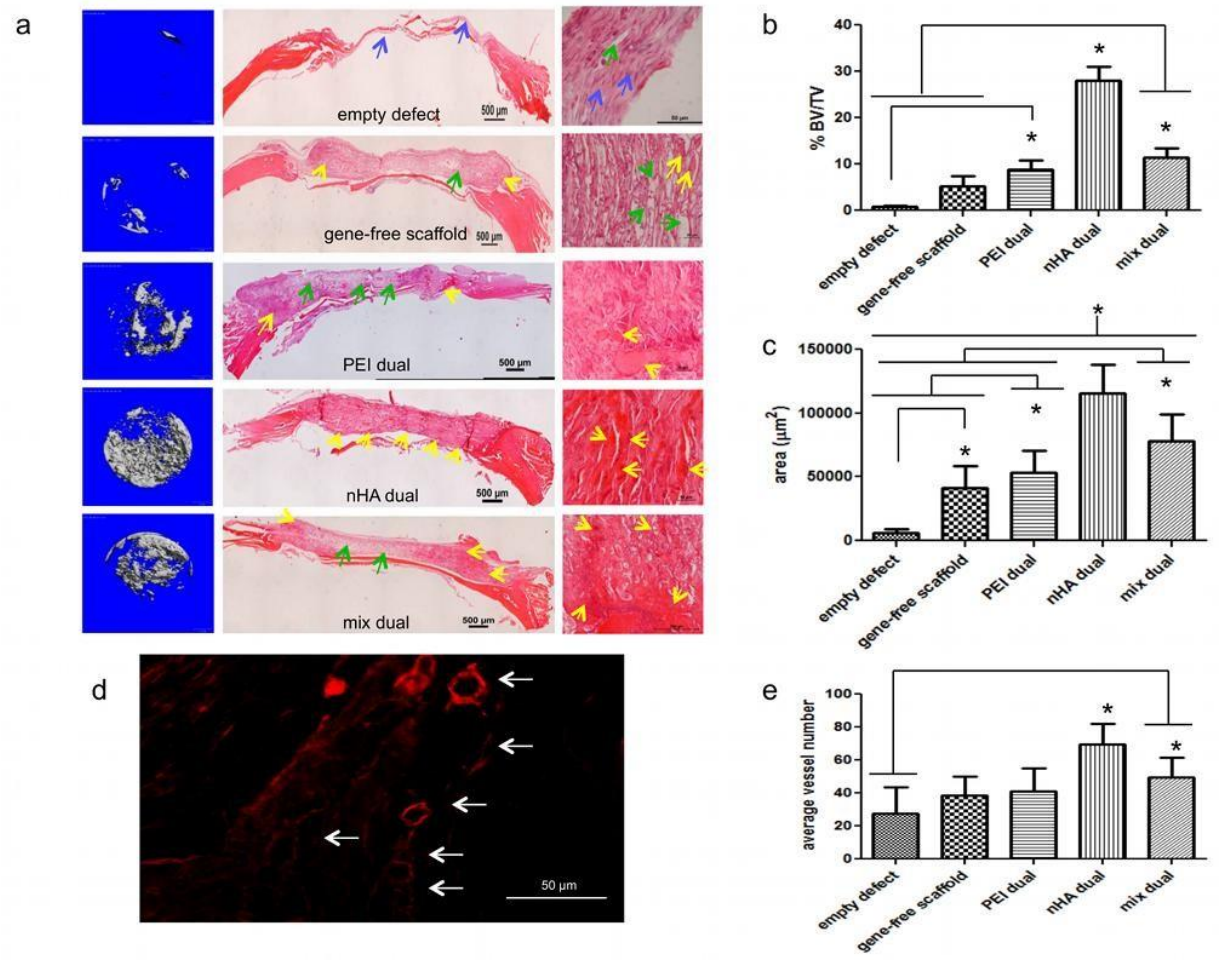

Figure 3. Enhanced bone repair and vessel formation in dual gene-activated scaffolds. a, Qualitative microCT analysis and macroscopic and high magnification images of H & E stained sections of each defect. All dual scaffolds displayed some degree of healing but the nHA dual scaffold promoted the highest levels of bone formation as demonstrated when b, microCT results were quantified. c, Quantitative histomorphometric analysis detailing the mean total area of bone nucleation sites corroborated these results. d, Representative image of CD31 positive vessels in defect. e, Quantification of vessel number revealed that the nHA dual scaffold had more vessels than any other group. * Blue arrows represent fibrotic regions, green arrows represent acellular regions, yellow arrows represent areas of new bone formation/bone nucleation sites/good integration with surrounding bone, white arrows represent CD31 stained vessels. *p ≤0.05

This study demonstrates accelerated bone regeneration through the combination of coll-nHA scaffold engineered specifically for bone repair with the sustained localised delivery of both an angiogenic and an osteogenic gene and represents a promising new concept in tissue engineering. The importance of vector choice was also shown to be essential. In gene therapy, high transfection

efficiencies are sought after but interestingly, even though nHA resulted in less cell-mediated protein production, the nHA dual scaffold ultimately demonstrated the greatest potential for enhancing *in vivo* bone formation. Furthermore, non-viral vectors are generally cited as relatively inefficient to their viral counterparts [19] meaning they are often disregarded in favour of viral vectors [20]. Herein, we have shown the therapeutic efficacy of using non-viral vectors in a 3D scaffold both *in vitro* and within a critical-size defect *in vivo* indicating that they should not be overlooked in the derivation of new therapeutics in the field. From a therapeutic perspective, all combinatorial dual gene-activated scaffolds were successful in increasing bone regeneration but markedly accelerated bone healing was observed in the nHA dual gene-activated scaffold. After only 4 weeks, a very early timepoint in the bone healing timeframe, rats treated with the nHA dual scaffold displayed complete bridging of the defect. Collectively, this study has underlined the potential of a series of non-viral gene-activated scaffolds in bone regeneration. Conclusively, the nHA dual scaffold emerged as a scaffold with immense potential in non-viral orthopaedic gene therapy.

Experimental Section

Refer to Supplementary Methods for more detailed descriptions.

Cell culture

MSCs, HUVECs, MC3T3-E1s were cultured using standard cell culture techniques as described in Supplementary Methods.

Plasmid propagation & Cell transfection

Plasmid amplifications were carried out by transforming One Shot® TOP10 Chemically Competent *E. coli* bacterial cells (Biosciences) according to the manufacturer's protocol and isolating pDNA using a Plasmid Maxi Kit (Qiagen). PEI [15] and nHA transfections [18] were carried out as detailed previously. Nucleofection was carried out as per manufacturer's instructions (Amaxa).

Enzyme-linked Immunosorbent Assay (ELISA) for BMP2 and VEGF quantification post transfection

The cell culture supernatant was collected and analysed by ELISA according to the manufacturer's instructions.

Gene-activated scaffold fabrication

The coll-nHA scaffold was fabricated and crosslinked as previously described [18]. PEI-pDNA complexes and nHA-pDNA nanoparticles were soak-loaded onto the scaffolds to form gene-activated scaffolds [15, 18].

Osteogenesis assays

Cells/scaffolds were cultured in osteogenic media consisting of DMEM supplemented with 10% FBS, 1% penicillin/streptomycin, 10mM β-glycerophosphate (Sigma-Aldrich), 50µm ascorbic acid 2-phosphate (Sigma-Aldrich) and 100nM dexamethasone (Sigma-Aldrich). Post-transfection, cells/scaffolds were assayed at 14 days for calcium deposition as a measure of osteogenesis using a Stanbio calcium assay (Calcium CPC Liquicolour, Stanbio Inc.) and DNA quantification was performed using a Quant-iT™ PicoGreen® dsDNA kit (Invitrogen). Scaffolds were qualitatively analysed *in vitro* using microcomputed tomography (Medical 40 MicroCT system, Scanco). Alizarin red staining was also performed on 7µm sections of the scaffolds.

Bioactivity analysis of BMP2 and VEGF produced by transfected MSCs

MSCs were transfected with PEI/nHA-pBMP2 and cultured in pre-osteoblast (MC3T3-E1) growth media. The conditioned media i.e. supernatant from transfected MSCs was applied to pre-osteoblasts in a 1:1 ratio with osteogenic media and an osteogenic assay was performed. Similarly, rMSCs were transfected with PEI/nHA-pVEGF and cultured in endothelial cell (HUVEC) growth media. The media from transfected rMSCs was applied to endothelial cells in a 1:1 ratio CM:fresh endothelial cell media. DNA quantification was performed as a measure of proliferation.

Surgical procedure

Ethical approval was given by the Research Ethics Committee of RCSI (REC Approval No. 662) and an animal license by the Department of Health of the Irish Government (Ref. B100/4416). A 7mm circular transosseous defect was created in the rat's cranium and the scaffolds were immediately inserted. Animals were sacrificed 1 or 4 weeks post-surgery by CO_2 asphyxiation. The defect area was resected for analysis.

Qualitative and quantitative analysis of bone healing using microCT

Scans and reconstructions were performed and bone repair was expressed as a percentage of bone volume over total volume (% BV/TV) within the defect area.

Histomorphometrical analysis of bone healing

Specimens were decalcified in 10% formic acid, bisected and embedded in paraffin wax blocks. 7µm sections were then cut, de-paraffinised, rehydrated through decreasing grades of alcohol, stained with haemotoxylin and eosin, dehydrated with increasing grades of alcohol, mounted and imaged. Areas of new bone formation were identified by deep pink staining and quantified by measuring their area in each section and calculating the mean total area per group.

Quantification of vessel formation

Histological sections were de-paraffinised, rehydrated, incubated in a primary mouse anti-rat CD31 antibody tagged with TRIT-C (BD) and mounted. 5 random sections were acquired for each sample, the amount of vessels in each section was collated and vessel quantification was presented as the mean value for the sum of these 5 sections.

Statistical Analysis

Results are expressed as the mean ± standard deviation. Statistical significance was generally assessed using One-way ANOVA with post hoc Holm-Sidak tests. Two-way ANOVA followed by post hoc Holm-Sidak tests were carried out in Figures 1b, 1c, & 1f. The sample size was n=3 for *in vitro* studies and n=8 for *in vivo* studies where $p \leq 0.05$ values were considered statistically significant.

Acknowledgements

This work was supported by the European Research Council under the European Community's Seventh Framework Programme (FP7/2007-2013) / ERC grant agreement n° 239685 and a Science Foundation Ireland, President of Ireland Young Researcher Award (04/Yl1/B531). Collagen was kindly provided by Integra LifeSciences Corporation and the pBMP2 plasmid was kindly donated by Kazihusa Bessho, Kyoto University, Japan.

References

[1] T. P. Richardson, M. C. Peters, A. B. Ennett, D. J. Mooney, *Nat. Biotechnol*. **2001**, *19*, 1029.

[2] R. T. Franceschi, *J. Dent. Res*. **2005**, *84*, 1093.

[3] D. H. Kempen, L. Lu, A. Heijink, T. E. Heffernan, L. B. Creemers, A. Maran, M. J. Yaszemski, W. J. Dhert, *Biomaterials*. **2009**, *30*, 2816.

[4] Z. S. Patel, S. Young, Y. Tabata, J. A. Jansen, M. E. K. Wong, A. G. Mikos, *Bone*. **2008**, *43*, 931.

[5] B. De la Riva, E. Sanchez, A. Hernandez, R. Reyes, F. Tamimi, E. Lopez-Cabarcos, A. Delgado, C. Evora, *J. Control. Release*. **2010**, *143*, 45.

[6] J. T. Koh, Z. Zhao, Z. Wang, I. S. Lewis, P. H. Krebsbach, R. T. Franceschi, *J. Dent. Res*. **2008**, *87*, 845.

[7] C. Zhang, K. Z. Wang, H. Qiang, Y. L. Tang, Q. Li, M. Li, X. Q. Dang, *Acta Pharmacol. Sin.* **2010**, *31*, 821.

[8] M. Zhao, Z. Zhao, J. T. Koh, T. Jin, R. T. Franceschi, *J. Cell Biochem*. **2005**, *95*, 1.

[9] A. Yamaguchi, T. Komori, T. Suda, *Endocr. Rev*. **2000**, *21*, 393.

[10] S. C. Gamradt, J. R. Lieberman, *Ann. Biomed. Eng*. **2004**, *32*, 136.

[11] E. V. van Gaal, R. van Eijk, R. S. Oosting, R. J. Kok, W. E. Hennink, D. J. Cromellin, E. Mastrobattista, *J. Control. Release.* **2011**, *154*, 218.

[12] J. M. Kanczler, P. J. Ginty, L. White, N. M. Clarke, S. M. Howdle, K. M. Shakesheff, R. O. Oreffo, *Biomaterials*. **2010**, *31*, 1242.

[13] Y. Shou, Z. Ma, T. Lu, B. P. Sorrentino, *PNAS*. **2006**, *103*, 11730.

[14] S. Hacein-Bey-Abina, C. von Kalle, M. Schmidt, F. Le Deist, N. Wulffraat, E. McIntyre, I. Radford, J. L. Villeval, C. C. Fraser, M. Cavazzana-Calvo, A. Fischer, *N. Engl J. Med*. **2003**, *348*, 255.

[15] E. G. Tierney, G. P. Duffy, A. J. Hibbitts, S. A. Cryan, F. J. O'Brien, *J. Control. Release*. **2012**, *158*, 304.

[16] E. G. Tierney, K.McSorley, C. L. Hastings, S. A. Cryan, T. O'Brien, M. J. Murphy, F. P. Barry, F. J. O'Brien, G. P. Duffy, *J. Control. Release*. **2013**, 165, 173.

[17] G. M. Cunniffe, G. R. Dickson, S. Partap, K. T. Stanton, F. J. O'Brien, *J. Mater. Sci. Mater. Med*. **2010**, *21*, 2293.

[18] C. M. Curtin, G. M. Cunniffe, F. G. Lyons, K. Bessho, G. R. Dickson, G. P. Duffy, F. J. O'Brien, *Adv. Mater*. **2012**, *24*, 749.

[19] T. N. Vo, F. K. Kasper, A. G. Mikos, *Adv. Drug Deliv. Rev*. **2012**, *64*, 1292.

[20] C. H. Evans, *Expert Rev. Mol. Med*. **2010**, *12*, 18.

Supporting Information

Click here to download Supporting Information: Supplementary Information.docx